INFLUENCING FACTORS OF METHANE FLUX IN A WARM-TEMPERATE MIXED PLANTATION OF NORTH CHINA UNDER PRECIPITATION

ZHUANG, J. J.[1] – ZHANG, J. Y.[2] – ZHANG, J. S.[3*]

[1]*School of Civil Engineering and Architecture, Xinxiang University, Xinxiang Henan 453003, China*

[2]*School of Biological Engineering, Xinxiang University, Xinxiang Henan 453003, China*

[3]*Research Institute of Forestry, Chinese Academy of Forestry, Beijing 100091, China*

**Corresponding author*
e-mail: zhuangjingnd@126.com; phone: +86-134-0373-1415

(Received 23rd Mar 2024; accepted 23rd Sep 2024)

Abstract. Examination of the effect of heavy rainfall on soil CH_4 fluxes could help to predict the feedback mechanism behind CH_4 fluxes in the global context. In this study, we used an automatic multichamber system in black locust (*Robinia pseudoacacia* L.) plantations in the hilly area of North China as the object for this study to observe CH_4 fluxes continuously before and after three rainfall events. Simultaneously, we monitored air temperature, relative humidity, solar radiation, soil temperature and soil moisture to consider the relationship between microenvironmental factors and CH_4 fluxes before and after rainfall. The results showed that: The inhibitory effect of heavy rainfall on soil CH_4 fluxes was dependent on the soil moisture status. The duration of the inhibitory effect during heavy rainfall in the wet season was longer than that during heavy rainfall after prolonged drought in the late growing season. A quadratic relationship was observed between soil CH_4 fluxes and soil temperature, while a linear relationship was observed between soil CH_4 fluxes and soil moisture. The key factors affecting soil CH_4 flux are different for different rainfall events. This study provides a scientific basis for the carbon budget of forest ecosystems in the studied region and a comprehensive assessment of the ecological functions of plantation forests.
Keywords: *precipitation event, carbon cycle, mixed plantation, key factors*

Introduction

Methane (CH_4) is the second-most important greenhouse gas after carbon dioxide (CO_2), which is a powerful greenhouse gas with a global warming potential more than 30 times higher than that of carbon dioxide (Ge et al., 2023). As the largest carbon reservoir in terrestrial ecosystems, forest ecosystems absorb about 14.2 ± 15.5 Tg of CH_4 annually, and the amount of CH_4 absorbed by forest soils accounts for 80% of the amount absorbed by natural soils that are not saturated with water (Tarasova et al., 2023). Thus, forest soil methane uptake capacity is one of the most important factors influencing changes in atmospheric methane concentrations.

Forest soils become a net sink or source of atmospheric methane, depending on the balance between aerobic methane oxidation and anaerobic methane decomposition of organic matter to generate methane (Xiong et al., 2024). Global climate models predict that changes in global precipitation patterns have resulted in increased precipitation at high latitudes, decreased precipitation in subtropical regions, and frequent droughts and extreme precipitation events (Roman et al., 2015; Trenberth, 2011), and that changes in precipitation affect soil aeration by altering soil water content, which in turn affects soil

http://www.aloki.hu ● ISSN 1589 1623 (Print) ● ISSN 1785 0037 (Online)
DOI: http://dx.doi.org/10.15666/aeer/2301_171188

CH_4 oxidation and generation processes, and thus soil CH_4 uptake rates. It is widely recognized that soil methane uptake capacity is negatively correlated with soil water content, mainly because increased soil water content hinders the diffusion of methane and oxygen from the air into the soil and reduces the substrate supply of methane-oxidizing bacteria in the soil, thus affecting the rate of soil methane uptake (Luo et al., 2013). Rainfall is not only a major source of soil moisture, but it also a key parameter regulating the exchange of energy and water between the atmosphere and land surface (Dong et al., 2022). As a result of the differences in rainfall patterns regionally, the availability of ecosystem water has changed at both short-term (hours or days) and long-term (seasonal and interannual) time scales (Jiao et al., 2021). Thus, the response of soil moisture is sensitive to changes in precipitation patterns, which are controlled by season, temperature, light, vegetation, soil texture and many other factors, thereby increasing uncertainties associated with estimating the rainfall effect on the soil CH_4 flux (Xu, 2023). Among all experiments, changes in the amount of precipitation were found to substantially stimulate (Petrakis et al., 2017), significantly inhibit (Sanaullah et al., 2012; Zhou, Zuo, and Smaill, 2021), or have no effect (Ni et al., 2019) on soil GHG fluxes. For example, the average CH_4 emissions decreased by approximately 82% as water draw down varied from 0 (0.94 mg CH_4 m^{-2} h^{-1}) to -50 cm (0.17 mg CH_4 m^{-2} h^{-1}) (Yang et al., 2022). The native forest was consistently the strongest CH_4 sink (-2.9 kg CH_4 -C ha^{-1} $year^{-1}$), while the pasture became a short-term CH_4 source after heavy rainfall when the soil reached saturation in subtropical Australia (Lona et al., 2018). However, the effects of altered precipitation patterns on methane uptake are still not concluded qualitatively or quantitatively and its occurrence mechanism is still unclear (Venturini et al., 2022; Zhou et al., 2021). China's warm-temperate continental monsoon climate is one of the largest and most distinctive climate types in the world, spanning more than 10 latitudes from north to south, and it is also the most sensitive region in response to global changes. Therefore, in-depth studies are needed on how changes in precipitation patterns will affect the ability of warm temperate forest soils to absorb methane and the mechanisms of their effects.

As an important forest resource reserve area in China, the forest ecosystems of North China mountains play an irreplaceable role in carbon sequestration and emission reduction, soil conservation, climate regulation, air purification, and maintenance of ecological balance (Yang et al., 2022). *Robinia pseudoacacia* has been one of the main silvicultural species in the ecological projects in the mountains of North China. As a nitrogen-fixing pioneer species, it can significantly improve soil structure, increase soil nutrients and soil erosion resistance, also it has a large ecological service function, and plays an important role in windbreak and sand fixation, hydrological regulation, and ditch fixation and slope protection, and it was once regarded as a promising afforestation tree (Song et al., 2018).

Based on these considerations, we selected *Robinia pseudoacacia* plantations as the object for this study of the effects of rainfall events on CH_4 fluxes. We used an automatic multichamber system to continuously observe environmental factors and CH_4 fluxes in situ during, before and after rainfall events. Our objectives in this study were as follows: (1) evaluating the effects of rainfall on CH_4 fluxes during drought and rainy periods in a temperate forest, (2) investigating the impact of soil hydrological changes (e.g., soil temperature and moisture) on CH_4 fluxes when rainfall occurs, (3) describing the relationship between soil temperature, soil moisture and CH_4 fluxes after rainfall, and (4) determining the key environmental factors explaining the effect of rainfall on CH_4 fluxes rates. The aim of this paper was to provide a theoretical basis for further evaluation of the impact of ecological engineering from forestry on the carbon cycle and climate change in the region.

Materials and methods

Site description

This study was conducted in a broad leaf dominant mixed plantation at the Xiaolangdi forest experimental site (35°01’ N, 112°28’ E; elevation 410 m). The station, a member of the Chinese Forest Ecosystem Research Network, is located in the hilly area of North China, adjacent to the south side of Taihang Mountain and north of the Yellow River (*Fig. 1*). This district is characterized by a warm-temperate continental monsoon climate. The annual mean precipitation is 641.7 mm, and 68.3% of the gross precipitation falls from June to September. The average monthly temperature ranges from 1.15°C in January to 24.19°C in July, with a mean annual temperature of 14.6°C. The annual average sunshine hours are 2367.7 h (Sun et al., 2014).

The soil parent material is composed of limestone, and the soil is mainly brown loam (Sun et al., 2014). The tree species in the mixed plantation are cork oak (*Quercus variabilis* blume), black locust (*Robinia pseudoacacia* L.) and arborvitae (*Platycladus orientalis*) (Tong et al., 2014). The sampling site (15 m × 15 m) was dominated by *Robinia psedudoacia* and *Grewia biloba* G. Don, with vegetation coverage of over 90%, average diameter at breast height of 10.8 cm and average height of 8.3 m.

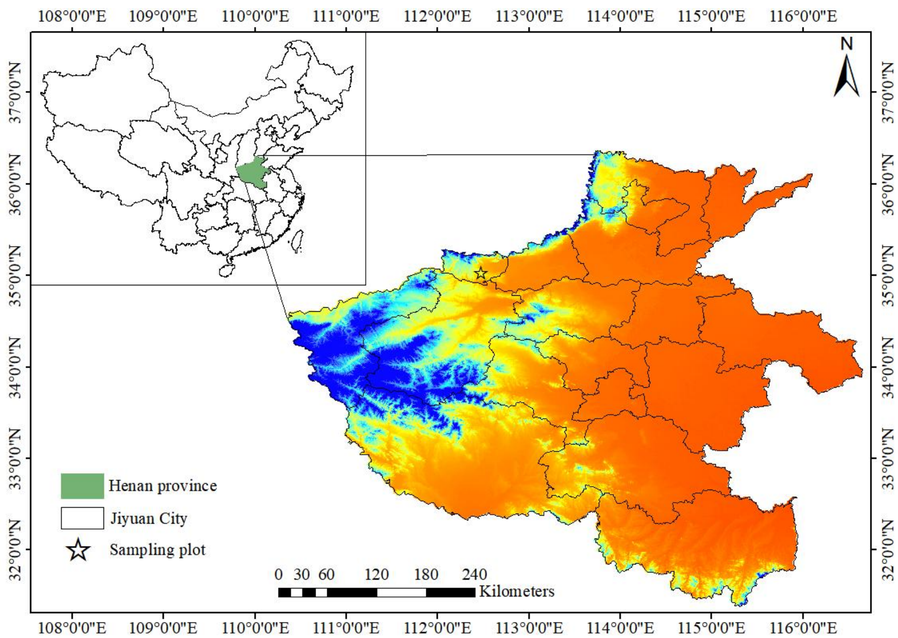

Figure 1. *Location of the Xiaolangdi mixed plantation site and the topography around the study site*

Measurement of CH_4 emissions

To study the effect of rainfall on the soil methane flux in hilly areas of North China, a monitoring campaign for collection of CH_4 emissions was carried out in the periods of March-May; June-August and September-November 2023. An automatic Greenhouse

http://www.aloki.hu ● ISSN 1589 1623 (Print) ● ISSN 1785 0037 (Online)
DOI: http://dx.doi.org/10.15666/aeer/2301_171188

Gas Analyzer (AGGA) (LGR 908-0011, Los Gatos Research Inc., USA), which used off-axis integrated-cavity output spectroscopy (laser spectrum technology), was used to measure the soil CH_4 concentration. The whole system consisted of three transportable chambers and a central data registry and control unit mounted on a modified trailer. This central unit contains a laser gas analyzer, a humidity trap and solenoid valves to change the gas flow to the specific chamber to be measured. The chambers were 0.17 m in height, with a volume of 3.10×10 m^3 and a measuring area of 3.14×10^{-3} m^2. The PVC (polyvinyl chloride polymer) collars (20 cm in inner diameter) were permanently inserted into the plot to a depth of 5-10 cm before the start of our measurements in December 2022 (*Fig. 2*). Air from the chambers passed through 10 m of tubing, with an internal diameter of 3 mm, to the analytical box. After the nondestructive analysis, the air was passed back into the chambers. Concentrations of CH_4 and water vapor and the air temperature inside the chambers were recorded. The chambers were equipped with a capillary tube to retain atmospheric pressure inside the chambers when sampling. The equipment was designed to automatically record the CH_4 concentration in the chamber head space every 1 s. For each measurement, the lid was sealed to the chamber and conditions were allowed to equilibrate for approximately 5 s. During the next 5 min, CH_4 concentrations within the chamber were measured, and an average CH_4 flux (F, $nmol \cdot m^{-2} \cdot s^{-1}$) was calculated using the following equation:

$$F = 10 \times \frac{VP_0 \times (1 - \frac{W_0}{1000000})}{RS \times (T_0 + 273.15)} \times \frac{\Delta c}{\Delta t} \qquad \text{(Eq.1)}$$

where F is the CH_4 flux of the soil ($nmol \cdot m^{-2} \cdot s^{-1}$); V is the volume of the gas channel (cm^3); P_0 is the standard state pressure (kPa); W_0 is the standard state water vapor concentration ($mmol \cdot mol^{-1}$); S is the cover area of gas chamber (cm^3); T_0 is the temperature of the standard state (°C); $\Delta c/\Delta t$ is the rate of increase of gas ($\mu mol^{-1} \cdot mol \cdot s^{-1}$); and R is the ideal gas constant (8.314 $Pa \cdot m^3 \cdot K^{-1} \cdot mol^{-1}$).

Figure 2. *Experimental layout and equipment in mixed plantation site*

The selected three rainfall events in the measured plots occurred on 1 April, 23 June and 6 October 2023. The first rainfall event ended at 23:00 on 4 April, with an accumulation of 35.4 mm. The second rainfall event started at 14:00 on 23 June and ended at 8:00 am on 28 June, with an accumulation of 136.1 mm. The third rainfall occurred at 9:00 am on 6 October and ended at 5:00 am on 7 October, with an accumulation of 23.4 mm.

http://www.aloki.hu ● ISSN 1589 1623 (Print) ● ISSN 1785 0037 (Online)
DOI: http://dx.doi.org/10.15666/aeer/2301_171188

Auxiliary measurements

Air temperature and relative humidity were measured with three shielded and aspirated HMP45 C sensors (Campbell Scientific Inc., Logan, UT, USA) at heights of 1.5 m above the soil surface. Solar radiation was measured with a quantum sensor (Model LI190SB, Li-cor, Inc., USA). In addition, soil temperature and soil moisture (Model 5TE, Decagon Devices Inc., USA) were continuously logged at depths of 0-10, 10-20 and 20-30 cm using AR5 (Avalon, Jersey City, NJ, USA) data loggers. Measurements at every soil layer depth were repeated 3 times. The measuring plots were permanent during the entire observation period. The mean data were stored at 10 min intervals. The meteorological data comes from a weather station 500 meters away from the experimental site.

In spring, summer and autumn, soil samples were collected by a soil auger from the sampling plots for physical and chemical analyses at depths of 0-10, 10-20 and 20-30 cm. In each subplot, three soil cores (3.5 cm in diameter) were taken, yielding 9 soil samples for each subplot and 45 soil samples for the study plot overall. The three samples were pooled, mixed to form one soil sample per sampling and sieved fresh on site through a 2 mm diameter sieve. The soils were then stored in an icebox and taken to the laboratory, and stored thereafter at 4°C for chemical analyses. Soil pH was determined in suspensions of a 1:5 ratio of soil to water, using a PHS-3C pH meter (Shanghai INESA Scientific Instrument Co. LTD, Shanghai, China). Total soil carbon was analyzed using the potassium dichromate oxidation method (HJ 615-2011, 2011), and soil nitrogen was measured by dry combustion (Multi EA® 5000, Elementar Analysensysteme, Hanau, Germany). The organic matter content was determined using the loss on ignition procedure (550°C, 8 h). Total P was measured spectrophotometrically (Shimadzu UV-2401PC) using the vanadomolybdate method. The ammonium-N and nitrate-N (NH_4^+-N and NO_3^--N) concentrations were measured using a flow injection auto-analyzer. All soil properties are listed in *Table 1*.

Table 1. *Soil physical and chemical properties in the 0-10, 10-20 and 20-30 cm layers (mean ± SD)*

Soil depth (cm)	pH	TC (g kg^{-1})	SOM (g kg^{-1})	TP (g kg^{-1})	NH_4^+-N (mg kg^{-1})	NO_3^--N (mg kg^{-1})
0-10	5.75 ± 0.35 a	1.87 ± 0.17 a	62.01 ± 52.87a	1.35 ± 0.39 a	43.87 ± 26.14 a	25.80 ± 10.24 a
10-20	5.75 ± 0.64 a	0.59 ± 0.36 b	14.32 ± 3.86 b	1.26 ± 0.06 a	34.99 ± 20.95 a	6.37 ± 1.87 b
20-30	6.35 ± 0.35 a	0.50 ± 0.15 b	11.81 ± 3.99 b	0.98 ± 0.03 a	32.42 ± 15.63 a	5.42 ± 1.36 b

TC, total carbon; TN, total nitrogen; SOM, soil organic matter; TP, total phosphorus. Values are presented as the mean ± standard deviation, and different letters in the same column indicate significant differences at $P < 0.05$

Statistical analysis

The statistical package SPSS 16.0 (SPSS Inc., Chicago, USA) was used for all statistical data processing. The significance of differences in soil properties among different soil depths in the plot was investigated using a one-way analysis of variance with Tukey's honest significant difference test. General linear modeling was used to identify the predictors of CH_4 fluxes in the different rainfall periods. Linear regression

http://www.aloki.hu ● ISSN 1589 1623 (Print) ● ISSN 1785 0037 (Online)
DOI: http://dx.doi.org/10.15666/aeer/2301_171188

analyses were used to determine the relationships between CH_4 fluxes and soil temperature soil and soil moisture. All analyses were evaluated using Origin Pro 2024 (OriginLab, Washington, USA).

Results

Environmental conditions

Large seasonal variations in precipitation and air temperature were observed in the study area (*Fig. 3; Table 2*). A total of 605.6 mm of rain fell at the site from October 2022 to October 2023, with clear wet and dry seasons. Several consecutive days of large rainfall totals during summer accounted for 61% of the seasonal totals.

Table 2. *Rainfall, soil moisture and temperature for each season in the lithoid hilly region of North China*

Months	Daily rainfall (mm)				Soil moisture (%)			Soil temperature (°C)		
	Number of rain days	Seasonal rain	Max daily	Mean daily	Mean	Max	Min	Mean	Max	Min
March-May	24	147.30	30.60	6.14	19.40	27.91	13.09	13.57	20.30	3.89
June-August	27	369.10	93.40	13.67	18.25	27.18	9.59	22.54	26.09	19.02
September-November	24	72.20	22.40	3.00	21.29	25.76	17.95	15.23	21.71	6.77
December-February	6	6.00	3.80	1.00	22.63	24.70	21.51	2.18	6.54	-0.35

The highest single daily rainfall amount was 93.4 mm on 3 August 2023. The frequent and often consecutive rainfall days and higher temperature during summer resulted in clear fluctuations in soil moisture (9.59% ~ 27.18%). Rainfall during winter was low and sporadic, with long-term drought stress in periods without rain resulting in a narrower fluctuation margin in soil moisture (21.51% ~ 24.70%) (*Table 2*). From winter to summer, the temperature ranged from a mean daily minimum of -3.91°C to over 27.47°C. The maximum air temperature was 27.47°C recorded on 28 July 2023, while the minimum air temperature was -3.91°C on 1 January 2023 (*Fig. 3*).

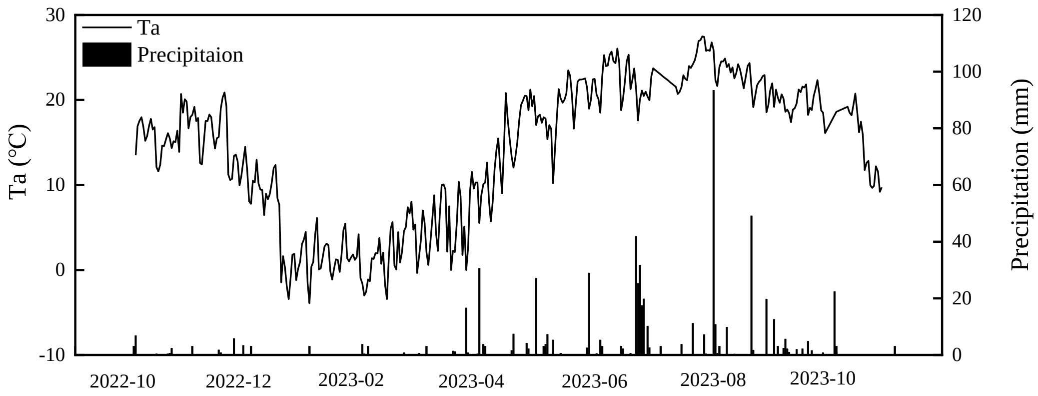

Figure 3. *Mean daily air temperature (Ta) and precipitation from 1 October 2022 to 15 October 2023 in the hilly region of North China*

http://www.aloki.hu ● ISSN 1589 1623 (Print) ● ISSN 1785 0037 (Online)
DOI: http://dx.doi.org/10.15666/aeer/2301_171188

Seasonal variation of CH_4 fluxes

There were clear seasonal variations in CH_4 fluxes at the sites during the growing and non-growing seasons. There was an increasing trend of CH_4 uptake from the early growing season (April) to the peak growing season (May) and a decreasing trend until the end of the growing season in October (*Fig. 4*). During the winter thaw–freeze and freeze–thaw periods, the daily variation in the CH_4 flux was pronounced. Measured CH_4 fluxes of soil ranged from -0.24 to -1.31 nmol·m^{-2}·s^{-1} and -0.48 to -1.55 nmol·m^{-2}·s^{-1}, with an average of -0.62 and -0.70 nmol·m^{-2}·s^{-1}, in the winter thaw–freeze and freeze–thaw periods, respectively. The maximum CH_4 uptake flux was -1.55 nmol·m^{-2}·s^{-1} in April, while the minimum CH_4 fluxes in soil (-0.24 nmol·m^{-2}·s^{-1}) occurred in February. As can be seen from *Figure 4*, Ms has a certain delay after the occurrence of rainfall, while Ts has a faster response speed to rainfall events.

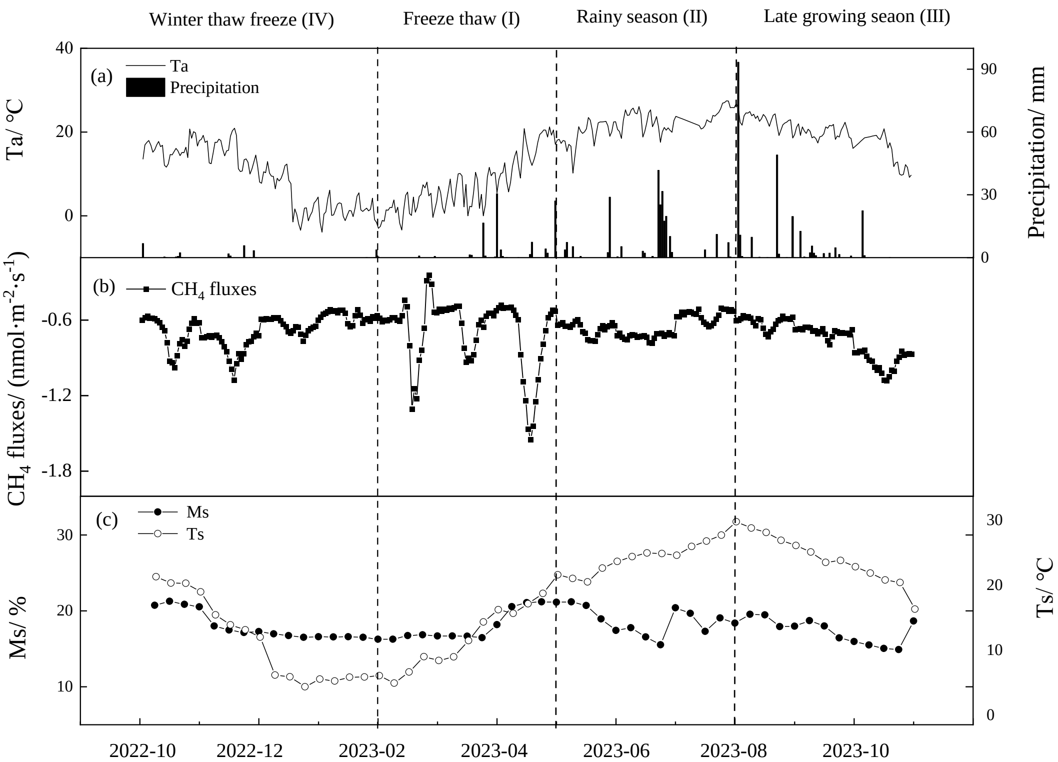

***Figure 4.** Diurnal variation of soil CH_4 fluxes from October 2022 to 15 October 2023 in the hilly region of North China*

Effect of rainfall on CH_4 fluxes, soil temperature and moisture

The diurnal variation of CH_4 fluxes, soil moisture and soil temperature before and after the rainfall events in April, June and October are shown in *Figures 5, 6* and *7*. The site was a net sink of atmospheric CH_4, ranging from -0.11 to -2.53 nmol·m^{-2}·s^{-1}, -0.13 to -1.19 nmol·m^{-2}·s^{-1} and -0.47 to -1.62 nmol·m^{-2}·s^{-1} in the April, June and October rainfall events, respectively. This shows that rain events only affected the size of the absorption capacity, without transformation from a net sink to a net source. Analysis of daily data (i.e., data averaged across a whole day) showed that before and after the rainfall had ceased, the CH_4 fluxes of soil presented daily change trend in a “V” shape.

http://www.aloki.hu ● ISSN 1589 1623 (Print) ● ISSN 1785 0037 (Online)
DOI: http://dx.doi.org/10.15666/aeer/2301_171188

The oxidation peak that occurred at noon each day suggests that the CH_4 absorption ability reached a maximum at this time (outside of rainfall periods).

The first rainfall event in the freeze–thaw period

There is no rain for a month before the first rainfall occurred. The gray area in *Figure 5* indicates the rainfall period from April 1 to April 4. After the rainfall event, the absorption capacity was lower than under no rainfall. Three days before the rainfall event, the average CH_4 fluxes of soil were -0.94 nmol·m^{-2}·s^{-1}. During the rainfall event, the average CH_4 fluxes were -0.68 nmol·m^{-2}·s^{-1}. Within 7 d after the rainfall event, with an average of -0.44 nmol·m^{-2}·s^{-1}, CH_4 fluxes decreased approximately twofold relative to the previous rainfall (*Fig. 5a*). After the rainfall event, the surface soil moisture and temperature changed, but there was no impact on deep soil (*Fig. 5b, c*). Three days after the rainfall, the average soil moisture content was 15.91%. After the rainfall event, soil moisture increased to 20.80%, and then gradually decreased within a 7 d period after the rainfall (*Fig. 5b*). The average soil temperature was 12.15°C within 7 d after rainfall, compared with 1.86°C before the rainfall (*Fig. 5c*). Before the rainfall event occurred, the CH_4 fluxes of soil were constrained by the lack of water. Rainfall only effectively supplied the soil moisture, and the period of oxidation restriction was short. Therefore, soil temperature may be an important factor affecting soil CH_4 fluxes during rainfall after prolonged drought periods.

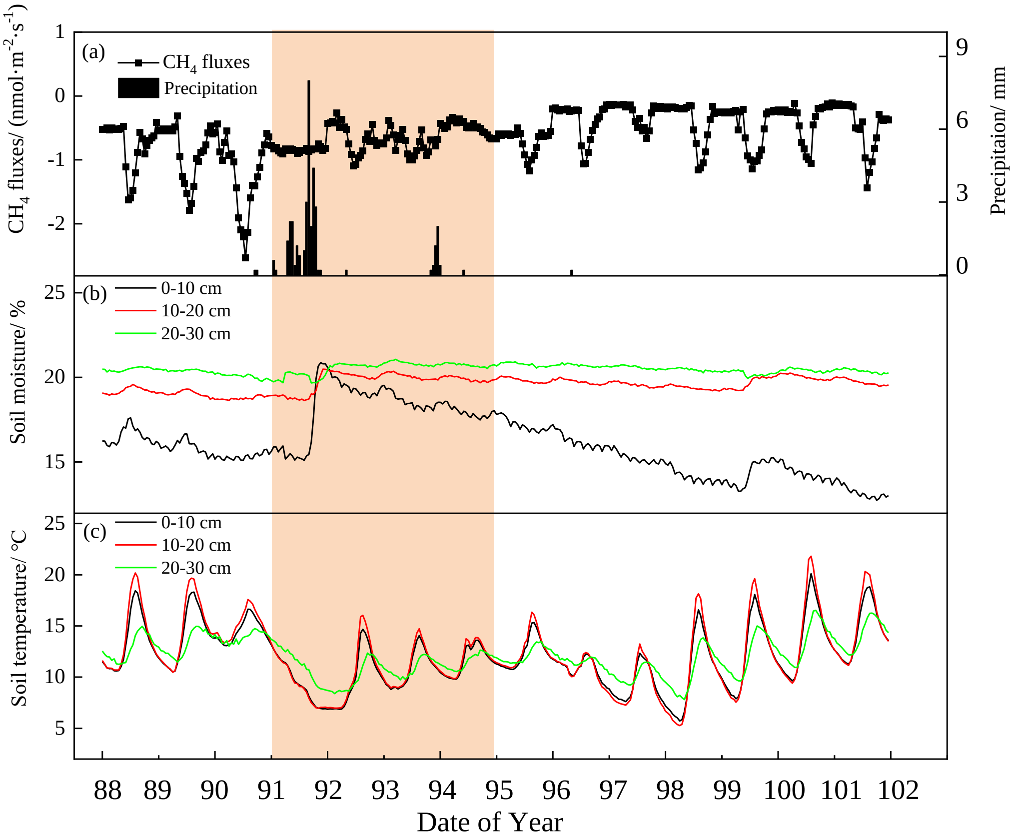

***Figure 5.** The CH_4 fluxes of soil superimposed with soil moisture and soil temperature at 0-10, 10-20, and 20-30 cm soil depths during the period before, during and after the first rainfall event (commencing April 1 with total amount 35.4 mm). Data represent the soil CH_4 fluxes (a), soil moisture (b) and soil temperature (c) in the hilly region of North China. The gray area indicates the duration of rainfall*

http://www.aloki.hu ● ISSN 1589 1623 (Print) ● ISSN 1785 0037 (Online)
DOI: http://dx.doi.org/10.15666/aeer/2301_171188

The second rainfall in rainy season

The second rainfall event on June 23 occurred approximately 2 months after the first rainfall event. Before the rainfall event occurred, there was a small-scale rainfall event each day, which caused an hourly average soil CH_4 flux rate of -1.04 nmol·m^{-2}·s^{-1}. After the rainfall ceased, the CH_4 fluxes of soil were -0.55 nmol·m^{-2}·s^{-1}, two times that before the rainfall event (*Fig. 6a*). In contrast with the first rainfall event, after the rain stopped, the downward trend in the oxidation capacity of soil was clear (*Figs. 5a* and *6a*). In the 4 d after the rain, the peak absorption occurred. The relative intensity of rainfall was larger than the first rainfall event and the average CH_4 fluxes of soil and soil temperature were smaller than the first rainfall event (*Fig. 6b*). However, as seen from *Figure 6b*, after the rainfall event, surface soil moisture reached a peak (33.56%) and CH_4 fluxes of soil gradually increased (-0.20 nmol·m^{-2}·s^{-1}). Compared with the first rainfall event, this rainfall had a greater impact on the deep soil. Soil moisture at 10-20 cm and 20-30 cm increased 7.99% and 7.69%, respectively (*Fig. 6b*). There was week-long continuous low absorption period, after which the oxidation capacity of the soil began to increase rapidly. The soil moisture amplitude of diurnal variation was 21.83%-33.56% in this period (*Fig. 6b*). After rainfall occurred, the soil temperature fluctuated immediately and tended to stabilize after 2 d (*Fig. 6c*). Therefore, the effect of summer heavy rainfall on soil oxidation capacity is clear, because of this long-term period of rainy weather.

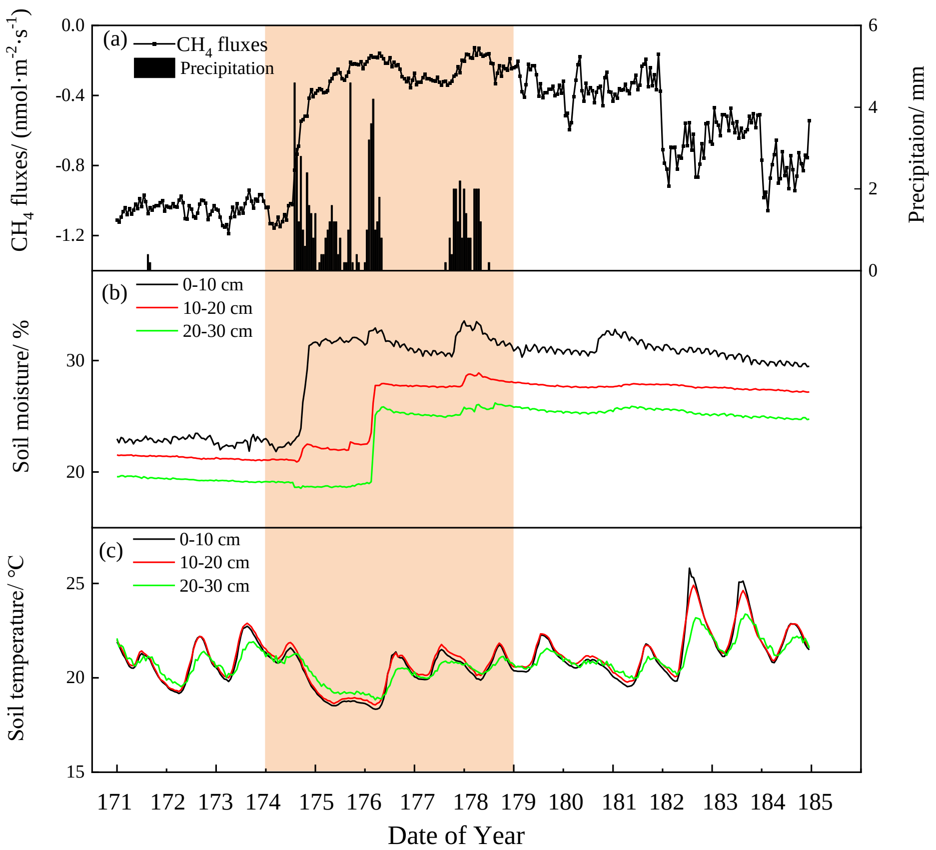

Figure 6. *Methane fluxes superimposed with soil moisture and soil temperature at 0-10, 10-20, and 20-30 cm soil depths during the period before, during and after the second rainfall event (commencing June 23 with total amount 136.1 mm). Data represent soil CH_4 fluxes (a), soil moisture (b) and soil temperature (c) in the hilly region of North China. The gray area indicates the duration of rainfall*

http://www.aloki.hu ● ISSN 1589 1623 (Print) ● ISSN 1785 0037 (Online)
DOI: http://dx.doi.org/10.15666/aeer/2301_171188

The third rainfall event in late growing season

The third rainfall event occurred on October 6. At this stage, the drought period affecting the soil has eased, and small-scale rainfall events occurred frequently. The third rainfall event lasted approximately 2 d, and the weather remained cloudy for 2 d after the rain ceased. Before the rainfall began, the average soil CH_4 flux was -1.01 nmol·m^{-2}·s^{-1}. During the rainfall process, the average soil CH_4 flux was -0.60 nmol·m^{-2}·s^{-1}, which represents a reduction of approximately 40% relative to before the rainfall. After the rainfall event, the average soil CH_4 flux was -0.93 nmol·m^{-2}·s^{-1}, a reduction of approximately 10% relative to before the rain (*Fig. 7*). Although the rainfall amount was small, soil moisture and temperature fluctuations were not significant between the first and second rainfall events. After the rainfall event, the soil moisture was 24.59% (*Fig. 7c*). This may be mainly due to the presence of a thick litter layer, which prevents water infiltration. The precipitation amount was minimal, and thus the soil moisture increase was correspondingly small. There was also a certain lag effect, which affected the oxidation capacity of soil and has a lag period. Soil temperature also showed a different trend to that observed for the first and second rainfall events. Before the rainfall commenced, the soil temperature range was 13.95-17.41°C. During the rainfall process, the soil temperature was 14.28-16.38°C, and this increased to 15.14-19.99°C after the rainfall ceased (*Fig. 7c*).

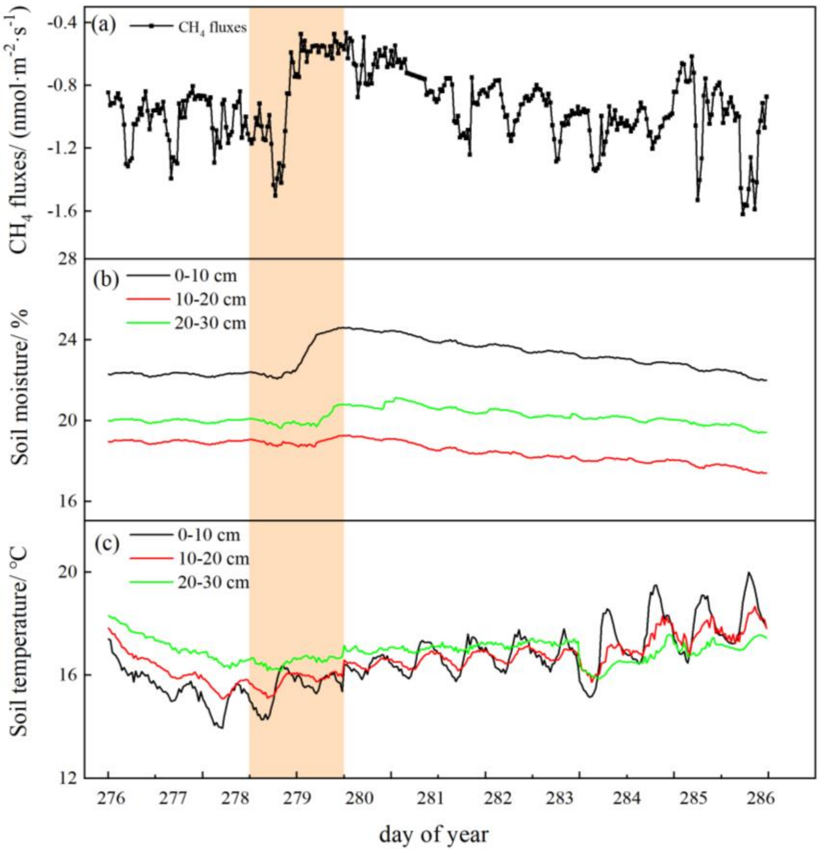

Figure 7. *Methane fluxes superimposed with soil moisture and soil temperature at 0-10, 10-20, and 20-30 cm soil depths during the period before, during and after the third rainfall event (commencing October 6 with a total amount of 23.4 mm). Data represent soil CH_4 fluxes (a), soil moisture (b) and soil temperature (c) in the lithoid hilly region of North China. The gray area indicates the duration of rainfall*

http://www.aloki.hu ● ISSN 1589 1623 (Print) ● ISSN 1785 0037 (Online)
DOI: http://dx.doi.org/10.15666/aeer/2301_171188

Relationships between CH_4 fluxes and soil temperature and moisture

Figure 8 reflected the response characteristics of soil CH_4 fluxes to soil temperature and soil moisture. The relationship can be described by a quadratic curve (*Fig. 8*). Daily CH_4 fluxes of the three rainfall events were correlated with daily soil temperature and exhibited a parabolic relationship ($r^2 = 0.287$, 0.096 and 0.226; $P < 0.001$, $P < 0.001$ and $P < 0.01$), while CH_4 fluxes were correlated with daily soil moisture and exhibited a linear relationship ($r^2 = 0.035$, 0.783 and 0.352; $P < 0.01$, $P < 0.01$ and $P < 0.001$).

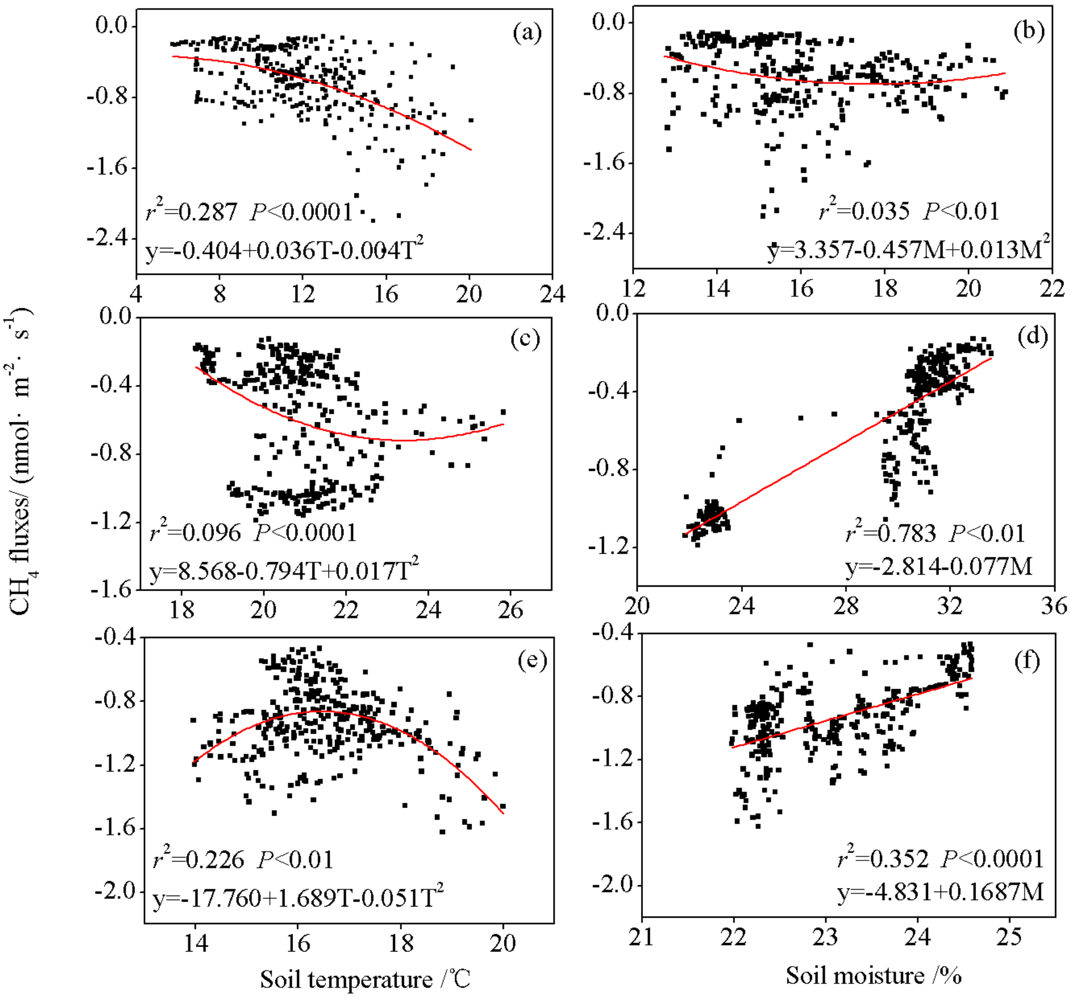

Figure 8. *Relationship between daily mean soil CH_4 fluxes with soil temperature (T, 5 cm soil depth) and soil moisture (M, 5 cm soil depth) in three rainfall events: relationship between CH_4 fluxes and T in the first rainfall event (a), in the second rainfall event (c), and in the third rainfall event (e); and relationship between CH_4 fluxes and M in the first rainfall event (b), in the second rainfall event (d), and in the third rainfall event (f), n = 336*

The turning point of the equation for the relationship between soil temperature and soil CH_4 fluxes can be calculated according to the quadratic equation. In the first rainfall event, when the value of the soil temperature was less than the inflection point (10°C), the increased soil temperature could promote the oxidation capacity of the soil. Conversely, when the value of the soil temperature was greater than the inflection point, the further increase in soil temperature could inhibit the oxidation capacity of soil

http://www.aloki.hu ● ISSN 1589 1623 (Print) ● ISSN 1785 0037 (Online)
DOI: http://dx.doi.org/10.15666/aeer/2301_171188

(*Fig. 8a*). During the second rainfall event, the inflection point of soil temperature was 22°C, and it was 17°C in the third rainfall event. In the first rainfall event, within a range of approximately 14 d, approximately 75.1% of the data were located to the right of the inflection point value (10°C) (*Fig. 8a*). In the second rainfall event, approximately 81.1% of the data were located to the left of inflection point value (22°C) (*Fig. 8c*). In the third rainfall event, almost all of the values were located to the left of the inflection point value (17°C) (*Fig. 8e*).

Before the first rainfall event, soil temperature was the limiting factor on the soil CH_4 flux when soil had been subjected to nearly a month of drought. Before the second rainfall event, the average level of soil moisture improved due to the continuously low rainfall, and soil moisture was in a relatively wet period. In the second rainfall event, the explanatory power of soil moisture on the soil CH_4 flux was considerably lower than that of the first and third rainfall events (*Fig. 8b*). The complex determination coefficient of the quadratic equation ($r^2 = 0.783$) was higher than that for the first ($r^2 = 0.035$) and third rainfall events ($r^2 = 0.352$) (*Fig. 8b, d, f*). This suggests that under relative moisture deficit conditions, the linear relationship can reflect the relationship between the soil CH_4 flux and soil moisture. However, in the case of low soil moisture, the linear relationship between soil moisture and CH_4 fluxes was weakened. For example, in the second rainfall event, the correlation between soil moisture and CH_4 fluxes was larger than that of the first and third rainfall events.

Therefore, rainfall after a prolonged drought (freeze–thaw), as well as continuous rainfall (rainy season) and rainfall after drought mitigation (late growing season) could inhibit the oxidation ability of soil as a whole. However, during the process of soil temperature and moisture change, the soil CH_4 flux may also inhibited when the soil temperature and moisture exceeded the inflection point (*Fig. 8b, d, f*).

Discussion

CH_4 flux

Generally, forests are usually regarded as important CH_4 sinks (Yu et al., 2017), and the soil CH_4 flux is known to exhibit a clear seasonal variation (Barrena et al., 2013). In our study, we found that the CH_4 uptake rate during the growing season was considerably higher than during the nongrowing season. The soil CH_4 flux was high in April and low in January (*Fig. 3*), which which is due to the fact that most methanotrophs in the aerobic zones of forest soils belong to medium temperature bacteria (Li and Zhang, 2010; Morishita et al., 2007). Our research results are consistent with Liu’s findings in northern and temperate forests in northern China and subalpine forests in southwest China, indicating that seasonal variation of soil temperature is the dominant factor to control CH_4 absorption (Liu et al., 2010). However, the seasonal fluctuations observed in our study contrasted with the results of for tropical China, which may be due to the warm and humid climate of the subtropical environment (Guo et al., 2023). Furthermore, because of the activities of below ground vegetation, other studies have also reported that the peaks of CH_4 uptake are usually recorded in winter and the lowest CH_4 uptake in summer (Chen et al., 2010; Li et al., 2010).

The continuous observation of the CH_4 flux before and after rainfall events has shown that the inhibition effect on the soil CH_4 flux was significant at the different rainfall intensities (*Figs. 5-7*). Our research has revealed that the CH_4 uptake at commencement of the rain suddenly decreased and soon returned to the level before the

http://www.aloki.hu ● ISSN 1589 1623 (Print) ● ISSN 1785 0037 (Online)
DOI: http://dx.doi.org/10.15666/aeer/2301_171188

rain. This is due to soil CH_4 fluxes are driven by soil aeration and redox controls on methanotrophy and methanogenesis (Wu et al., 2020). The rainfall event changes the soil moisture and decreases the soil O_2 level, which limits the growth and activity of methanotrophs in soil (Luo et al., 2013). Two forms of CH_4 oxidation have been recognized in soils: high affinity oxidation and low affinity oxidation (Yu et al., 2017). Some studies have indicated that CH_4 emissions increase significantly after rainfall (Lohila et al., 2016; Voigt et al., 2023). One study reported that, after rainfall, soil CH_4 emissions increased up to 2 times compared to before the rain occur in wetland and paddies (Cai, 2011). This may be because soil moisture and temperature could cause the number of methanotrophs to increase after rainfall in an aerobic microbial process (Qi et al., 2022). In our study, the first rainfall event occurred after a prolonged drought. Although rainfall increased the soil moisture, the period of the rainfall effect in the second rainfall (rainy season) was longer than that of the first rainfall event. This is mainly due to the relatively low moisture and temperature of air and soil during the dry season, which limited the activity of methanogens (Wu et al., 2020). The third rainfall event occurred in October 2015. During this period, there was a substantial increase to the amount of litter, and the litter layer added considerable thickness to the soil, which may have limited the diffusion of atmospheric O_2 to the soil (Qi et al., 2022), thus reducing the oxidation rate of soil CH_4. Furthermore, rainfall occurrence decreased the air temperature and removed the mechanism of soil moisture evaporation. Since the diffusion rate of CH_4 molecules in water is 10^{-4} times lower than that in air, this may have limited the metabolism of CH_4 oxidative bacteria or promoted the methanogenic process of methanogens, finally inhibiting CH_4 uptake in soil (Blankinship et al., 2010).

Relative contributions of soil moisture and temperature to the soil CH_4 flux

The soil CH_4 flux is usually regulated by the interaction of multiple factors; this effect is not a simple direct influence but is based on the interaction between environmental factors and thus has indirect effects on the soil CH_4 flux. Therefore, to identify the important environmental variables controlling the CH_4 flux of soil during the three rainfall events, a general linear model was applied to the hourly averaged CH_4 flux. The results of the single variable model for each of the rainfall events are shown in *Tables 3-5*. In the first rainfall event, before the rainfall commenced, soil temperature and air temperature explained more than 90% of the observed variability in CH_4 fluxes. After the rainfall event, surface soil temperature and moisture presented a slightly higher explanatory power for the CH_4 fluxes (*Table 3*). During the second rainfall event, soil temperature and air temperature were also key factors explaining the CH_4 flux of soil. After the rainfall event, soil moisture (5 cm depth) and air temperature explained more than 80% of the variability in CH_4 fluxes (*Table 4*). This shows that soil moisture was the main factor affecting the CH_4 flux of soil when the rainfall amount is large. In the third rainfall event, soil temperature (5 cm depth) and air temperature explained more than 95% of the CH_4 flux in the soil (*Table 5*). After the rainfall event, air temperature and global radiation were the main factors controlling CH_4 fluxes. This may be because litter reduced the water retention, and solar radiation influenced the temperature rise, which affects the CH_4 flux. Our research results show that the rainfall events significantly reduced the CH_4 fluxes of soil, and the larger CH_4 flux reductions occurred during the process of rainfall. As shown in *Figures 5-7*, the CH_4 fluxes of soil before rainfall and after the rainfall show a significant convex trend during the rainfall process.

http://www.aloki.hu ● ISSN 1589 1623 (Print) ● ISSN 1785 0037 (Online)
DOI: http://dx.doi.org/10.15666/aeer/2301_171188

Table 3. *Single variable general linear model results for the CH_4 fluxes (the first rainfall event), divided into before rainfall (29 March to 31 March 2015) and after rainfall (1 April to 11 April 2015), where T refers to temperature and M refers to moisture*

CH_4 fluxes	Before the rainfall				After the rainfall			
	Variable	r^2	**F-ratio**	***P*-value**	**Variable**	r^2	**F-ratio**	***P*-value**
	Soil T (0-10 cm)	1.000	106.506	0.077	Soil T (0-10 cm)	0.927	2.093	0.004
	Soil T (10-20 cm)	1.000	52.087	0.000	Soil T (10-20 cm)	0.920	1.372	0.160
	Soil T (20-30 cm)	0.920	1.884	0.138	Soil T (20-30 cm)	0.827	0.989	0.538
	Soil M (0-10 cm)	0.841	1.190	0.383	Soil M (0-10 cm)	0.807	1.182	0.229
	Soil M (10-20 cm)	0.766	1.474	0.162	Soil M (10-20 cm)	0.508	1.156	0.202
	Soil M (20-30 cm)	0.677	1.068	0.443	Soil M (20-30 cm)	0.484	1.746	0.001
	Solar radiation	0.929	12.037	0.000	Solar radiation	0.703	2.245	0.000
	Air temperature	0.992	5.486	0.092	Air temperature	0.917	1.219	0.281
	Relative humidity	0.990	5.910	0.047	Relative humidity	0.655	1.543	0.007

Table 4. *Single variable general linear model results for the CH_4 fluxes (the second rainfall event), divided into before rainfall (20 June to 22 June 2023) and after rainfall (23 June to 7 July 2023), where T refers to temperature and M refers to moisture*

CH_4 fluxes	Before the rainfall				After the rainfall			
	Variable	r^2	**F-ratio**	***P*-value**	**Variable**	r^2	**F-ratio**	***P*-value**
	Soil T (0-10 cm)	0.960	2.203	0.160	Soil T (0-10 cm)	0.727	1.101	0.288
	Soil T (10-20 cm)	0.897	0.951	0.595	Soil T (10-20 cm)	0.726	1.281	0.065
	Soil T (20-30 cm)	0.853	0.841	0.682	Soil T (20-30 cm)	0.673	1.227	0.097
	Soil M (0-10 cm)	0.711	0.966	0.558	Soil M (0-10 cm)	0.901	3.165	0.000
	Soil M (10-20 cm)	0.716	1.955	0.028	Soil M (10-20 cm)	0.839	4.810	0.000
	Soil M (20-30 cm)	0.671	1.773	0.049	Soil M (20-30 cm)	0.796	2.967	0.000
	Solar radiation	0.525	0.961	0.550	Solar radiation	0.551	1.118	0.229
	Air temperature	0.995	2.850	0.444	Air temperature	0.881	1.197	0.223
	Relative humidity	0.989	1.259	0.624	Relative humidity	0.741	3.635	0.000

Table 5. *Single variable general linear model for the CH_4 fluxes (the third rainfall event), divided into before rainfall (3 October to 5 October 2023) and after rainfall (6 October to 16 October 2023), where T refers to temperature and M refers to moisture*

CH_4 fluxes	Before the rainfall				After the rainfall			
	Variable	r^2	**F-ratio**	***P*-value**	**Variable**	r^2	**F-ratio**	***P*-value**
	Soil T (0-10 cm)	0.824	0.768	0.750	Soil T (0-10 cm)	0.821	1.898	0.001
	Soil T (10-20 cm)	0.855	0.751	0.755	Soil T (10-20 cm)	0.730	1.481	0.019
	Soil T (20-30 cm)	0.800	1.163	0.385	Soil T (20-30 cm)	0.522	1.362	0.038
	Soil M (0-10 cm)	0.804	1.498	0.167	Soil M (0-10 cm)	0.564	1.121	0.259
	Soil M (10-20 cm)	0.571	0.920	0.605	Soil M (10-20 cm)	0.440	1.794	0.001
	Soil M (20-30 cm)	0.546	1.043	0.453	Soil M (20-30 cm)	0.518	2.369	0.000
	Solar radiation	0.971	3.087	0.078	Solar radiation	0.890	1.806	0.008
	Air temperature	0.998	6.630	0.301	Air temperature	0.912	1.039	0.483
	Relative humidity	1.000	0.000	0.000	Relative humidity	0.820	1.653	0.008

http://www.aloki.hu ● ISSN 1589 1623 (Print) ● ISSN 1785 0037 (Online)
DOI: http://dx.doi.org/10.15666/aeer/2301_171188

The relationship between the rate of soil CH_4 uptake and soil temperature and moisture have been demonstrated in several field and laboratory studies (Feng et al., 2023; Wu et al., 2020). Our study showed a significant positive correlation between CH_4 uptake and soil temperature at the 0-10 cm soil depth before the rainfall in the three rainfall events (*Fig. 8*). The main reason was the surface soil temperature was strongly affected by the atmospheric temperature. In the surface soil, the CH_4 oxidizing bacteria are mesophilic microbes. The soil temperature influences the microbial activity, thereby affecting forest soil CH_4 oxidation (Qi et al., 2022; Wu et al., 2020; Xu, 2023). In our study, soil CH_4 uptake decreased as temperature increased or decreased from 10°C (inflection point) in the first rainfall event, and 22 and 17°C during the second and third rainfall events, respectively (*Fig. 8*). This was consistent with other results that indicated that the daily CH_4 uptake was related to temperature at 5 cm in soil depth in steppe and temperate forest environments (Wu et al., 2020). These variable results concerning the relationship between soil CH_4 uptake and soil temperature indicate that the soil CH_4 uptake is a complex process, which is influenced by multiple factors.

In our study, we found that CH_4 uptake had a linear relationship with soil moisture in three rainfall events ($r^2 = 0.021$, 0.768 and 0.133; $P < 0.01$, $P < 0.01$ and $P < 0.001$). The reason for this phenomenon is suppression of CH_4 uptake may be by physiological water stress of methanotrophs or CH_4 diffusion and O_2 transport (Blankinship et al., 2010; Rong et al., 2015). In the third rainfall event, after the rainfall had ceased, the capacity of CH_4 uptake was limited for longer than after the first and second rainfall events, even though the third rainfall event was smaller (*Figs. 4-6*). This was because at the end of the growing season, the litter layer limited water transfer with the atmosphere and the water retention caused a decrease in the CH_4 uptake (Li and Zhang, 2010). The litter layer may serve as a moisture-induced bidirectional buffer for atmospheric CH_4 uptake by forest soils (Wang et al., 2013). This may explain the finding that the limited effect of rainfall on CH_4 uptake was longer after the third rainfall event than after the first and second rainfall events (*Figs. 4-6*). In the second and third rainfall events, we found promotion of the oxidation capacity of CH_4 in soil after the rainfall ceased. This is because the drought limited CH_4 oxidizing bacteria and enzyme activity, and the reintroduction of moisture restored their activity, thereby promoting oxidation of CH_4 in soil (Feng et al., 2023).

Conclusions

Our study site, located in the rocky hilly area of northern China, was a sink for atmospheric CH_4, with an average uptake flux of -0.67 $nmol \cdot m^{-2} \cdot s^{-1}$ during the whole year. The occurrence of rainfall significantly reduced the oxidation ability of the soil in study area. The inhibitory effect of heavy rainfall on soil CH_4 fluxes depended on the soil moisture status. A quadratic relationship was observed between soil CH_4 fluxes and soil temperature, while a linear relationship was observed between soil CH_4 fluxes and soil moisture. Before the three rainfall events, soil temperature and air temperature were the key factors controlling the soil CH_4 flux. After the rainfall events, surface soil temperature and moisture, soil moisture (at a 5 cm depth), air temperature and global radiation were the main factors affecting the CH_4 flux of soil in the three rainfall events.

Acknowledgements. This work was financed by the Henan Provincial Science and Technology Tackling Project [grant number 242102320334].

REFERENCES

[1] Barrena, I., Menendez, S., Dunabeitia, M., Merino, P., Stange, C. F., Spott, O., Gonzalez-Murua, C., Estavillo, J. M. (2013): Greenhouse gas fluxes (CO_2, N_2O and CH_4) from forest soils in the Basque country: comparison of different tree species and growth stages. – Forest Ecology and Management 310: 600-611. DOI: 10.1016/j.foreco.2013.08.065.

[2] Blankinship, J. C., Brown, J. R., Dijkstra, P., Allwright, M. C., Hungate, B. A. (2010): Response of terrestrial CH_4 uptake to interactive changes in precipitation and temperature along a climatic gradient. – Ecosystems 13(8): 1157-1170. DOI: 10.1007/s10021-010-9391-9.

[3] Cai, Z. C. (2011): Greenhouse gas budget for terrestrial ecosystems in China. – Science China Earth Sciences 55(2): 173-182. DOI: 10.1007/s11430-011-4309-8.

[4] Chen, W. W., Wolf, B., Yao, Z. S., Brüggemann, N., Butterbach-Bahl, K. (2010): Annual methane uptake by typical semiarid steppe in Inner Mongolia. – Journal of Geophysical Research 115(15): 1-10. DOI: 10.1029/2009JD013783.

[5] Dong, X. F., Lai, X., Wang, Y. S., Dong, W., Zhu, J., Dong, L., Cen, S. X. (2022): Applicability evaluation of multiple sets of soil moisture data on the Tibetan Plateau. – Frontiers in Earth Science 10: 1-10. DOI: 10.3389/feart.2022.872413.

[6] Feng, H. L., Guo, J. H., Peng, C. H., Ma, X. H., Kneeshaw, D., Chen, H., Liu, Q. Y., Liu, M. Y., Hu, C., Wang, W. F. (2023): Global estimates of forest soil methane flux identify a temperate and tropical forest methane sink. – Geoderma 429: 116239. DOI: 10.1016/j.geoderma.2022.116239.

[7] Ge, M. Y., Korrensalo, A., Laiho, R., Kohl, L., Lohila, A., Pihlatie, M., Li, X. F., Laine, A. M., Anttila, J., Putkinen, A. (2023): Plant-mediated CH_4 exchange in wetlands: a review of mechanisms and measurement methods with implications for modelling. – Science of the Total Environment: 169662. DOI: 10.1016/j.scitotenv.2023.169662.

[8] Guo, J. H., Feng, H. L., Peng, C. H., Chen, H., Xu, X., Ma, X. H., Li, L., Kneeshaw, D., Ruan, H. H., Yang, H. Q. (2023): Global climate change increases terrestrial soil CH_4 emissions. – Global Biogeochem Cycles 37(1): e2021GB007255. DOI: 10.1029/2021GB007255.

[9] Jiao, W. Z., Wang, L. X., Smith, W. K., Chang, Q., Wang, H. L., D'Odorico, P. (2021): Observed increasing water constraint on vegetation growth over the last three decades. – Nature Communications 12(1): 3777. DOI: 10.1038/s41467-021-24016-9.

[10] Li, H. F., Zhang, X. F. (2010): Soil greenhouse gases emission from an Acacia crassicarpa plantation under effects of understory removal and cassia alata addition. – Chinese Journal of Applied Ecology 21(3): 563-568.

[11] Li, Y. Y., Dong, S. K., Liu, S. L., Zhou, H. K., Wu, X. Y. (2015): Seasonal changes of CO_2, CH_4 and N_2O fluxes in different types of alpine grassland in the Qinghai-Tibetan Plateau of China. – Soil Biology & Biochemistry 80: 306-314. DOI: 10.1016/j.soilbio.2014.10.026.

[12] Liu, S., Wang, C. K., Xu, F. (2010): Soil effluxes of carbon dioxide, methane and nitrous oxide during non-growing season for four temperate forests in northeastern China. – Acta Ecologica Sinica 30(15): 4075-4084.

[13] Lohila, A., Aalto, T., Aurela, M., Hatakka, J., Tuovinen, J. P., Kilkki, J., Penttila, T., Vuorenmaa, J., HaNninen, P., Sutinen, R. (2016): Large contribution of boreal upland forest soils to a catchment-scale CH_4 balance in a wet year. – Geophysical Research Letters 43(6): 2946-2953. DOI: 10.1002/2016GL067718.

[14] Lona, V. D., David, W. R., Clemens, S., Daniele, D. R., Peter, R. G. (2018): Effect of urbanization on soil methane and nitrous oxide fluxes in subtropical Australia. – Global Change Biology 24(12): 5695-5707. DOI: 10.1111/gcb.14444.

[15] Luo, G. J., Kiese, R., Wolf, B., Butterbach-Bahl, K. (2013): Effects of soil temperature and moisture on methane uptakes and nitrous oxide emissions across three different ecosystem types. – Biogeosciences 10(5): 3205-3219. DOI: 10.5194/bg-10-3205-2013.

http://www.aloki.hu ● ISSN 1589 1623 (Print) ● ISSN 1785 0037 (Online)
DOI: http://dx.doi.org/10.15666/aeer/2301_171188

[16] Morishita, T., Sakata, T., Takahashi, M., Ishizuka, S., Umata, H. (2007): Methane uptake and nitrous oxide emission in Japanese forest soils and their relationship to soil and vegetation types. – Soil Science and Plant Nutrition 53(5): 678-691. DOI: 10.1111/j.1747-0765.2007.00181.x.
[17] Ni, X. Y., Liao, S., Wu, F. Z., Groffman, P. M. (2019): Short-term precipitation pulses stimulate soil CO_2 emission but do not alter CH_4 and N2O fluxes in a northern hardwood forest. – Soil Biology and Biochemistry 130: 8-11. DOI: 10.1016/j.soilbio.2018.11.021.
[18] Petrakis, S., Seyfferth, A., Kan, J. J., Inamdar, S., Vargas, R. (2017): Influence of experimental extreme water pulses on greenhouse gas emissions from soils. – Biogeochemistry 133: 147-164. DOI: 10.1007/s10533-017-0320-2.
[19] Qi, Q., Zhao, J. S., Tian, R. M., Zeng, Y. F., Xie, C. Y., Gao, Q., Dai, T. J., Wang, H., He, J. S., Konstantinidis, K. T. (2022): Microbially enhanced methane uptake under warming enlarges ecosystem carbon sink in a Tibetan alpine grassland. – Global Change Biology 28(23): 6906-6920. DOI: 10.1111/gcb.16444.
[20] Roman, J., Knuteson, R., Ackerman, S., Revercomb, H. (2015): Predicted changes in the frequency of extreme precipitable water vapor events. – Journal of Climate 28: 7057-7070. DOI: 10.1175/JCLI-D-14-00679.1.
[21] Rong, Y. P., Ma, L., Johnson, D. A. (2015): Methane uptake by four land-use types in the agro-pastoral region of northern China. – Atmospheric Environment 116: 12-21. DOI: 10.1016/j.atmosenv.2015.06.003.
[22] Sanaullah, M., Chabbi, A., Rumpel, C., Kuzyakov, Y. (2012): Carbon allocation in grassland communities under drought stress followed by ^{14}C pulse labeling. – Soil Biology and Biochemistry 55: 132-139. DOI: 10.1016/j.soilbio.2012.06.004.
[23] Song, W. C., Tong, X. J., Zhang, J. S., Meng, P., Li, J. (2018): How a root-microbial system regulates the response of soil respiration to temperature and moisture in a plantation. – Polish Journal of Environmental Studies 27(6): 2749-2756. DOI: 10.15244/pjoes/81271.
[24] Sun, S. J., Meng, P., Zhang, J. S., Wan, X. C., Zheng, N., He, C. X. (2014): Partitioning oak woodland evapotranspiration in the rocky mountainous area of North China was disturbed by foreign vapor, as estimated based on non-steady-state $_{18}O$ isotopic composition. – Agricultural and Forest Meteorology 184: 36-47. DOI: 10.1016/j.agrformet.2013.08.006.
[25] Tong, X., Zhang, J., Meng, P., Zheng, N. (2014): Ecosystem water use efficiency in a warm-temperate mixed plantation in the North China. – Journal of Hydrology 512: 221-228. DOI: 10.1016/j.jhydrol.2014.02.042.
[26] Trenberth, K. E. (2011): Changes in precipitation with climate change. Climate change research. – Climate Research 47: 123-138. DOI: 10.3354/cr00953.
[27] Venturini, A. M., Dias, Naissa, M. S., Gontijo, J. B., Yoshiura, C. A., Paula, F. S., Meyer, K. M., Nakamura, F. M., Frana, A. G. D., Borges, C. D., Barlow, J. (2022): Increased soil moisture intensifies the impacts of forest-to-pasture conversion on methane emissions and methane-cycling communities in the eastern amazon. – Environmental Research 212(Pt A): 113139. DOI: 10.1016/j.envres.2022.113139.
[28] Voigt, C., Virkkala, A. M., Gosselin, G. H., Bennett, K. A., Black, T. A., Detto, M., Chevrier-Dion, C., Guggenberger, G., Hashmi, W., Kohl, L. (2023): Arctic soil methane sink increases with drier conditions and higher ecosystem respiration. – Nature Climate Change 13: 1095-1104. DOI: 10.1038/s41558-023-01785-3.
[29] Wang, Y. D., Wang, H. M., Ma, Z. Q., Dai, X. Q., Wen, X. F., Liu, Y. F., Wang, Z. L. (2013): The litter layer acts as a moisture-induced bidirectional buffer for atmospheric methane uptake by soil of a subtropical pine plantation. – Soil Biology & Biochemistry 66: 45-50. DOI: 10.1016/j.soilbio.2013.06.018.
[30] Wu, G., Chen, X. M., Ling, J., Li, F., Li, F. Y., Peixoto, L., Wen, Y., Zhou, S. L. (2020): Effects of soil warming and increased precipitation on greenhouse gas fluxes in spring

http://www.aloki.hu ● ISSN 1589 1623 (Print) ● ISSN 1785 0037 (Online)
DOI: http://dx.doi.org/10.15666/aeer/2301_171188

maize seasons in the North China Plain. – Science of the Total Environment 734: 139269. DOI: 10.1016/j.scitotenv.2020.139269.

[31] Xiong, J., Wang, G. X., Sun, X. Y., Hu, Z. Y., Li, Y., Sun, J. Y., Zhang, W., Sun, S. Q. (2024): Effects of litter and root inputs on soil CH_4 uptake rates and associated microbial abundances in natural temperature subalpine forests. – Science of the Total Environment 912: 168730.

[32] Xu, X. K. (2023): Effect of changes in throughfall on soil respiration in global forest ecosystems: a meta-analysis. – Forests 14(5): 1037. DOI: 10.3390/f14051037.

[33] Yang, Y. H., Shi, Y., Sun, W. J., Chang, J. F., Zhu, J. X., Chen, L. Y., Wang, X., Guo, Y. P., Zhang, H. T., Yu, L. F. (2022): Terrestrial carbon sinks in China and around the world and their contribution to carbon neutrality. – Science China Life Sciences 65: 861-895. DOI: 10.1007/s11427-021-2045-5.

[34] Yu, L. J., Huang, Y., Zhang, W., Li, T. T., Sun, W. J. (2017): Methane uptake in global forest and grassland soils over the period 1981-2010. – Science of the Total Environment 607-608: 1163-1172. DOI: 10.1016/j.scitotenv.2017.07.082.

[35] Zhou, X. Q., Zuo, H. L., Smaill, S. J. (2021): Incorporation of NPP into forest CH_4 efflux models. – Trends Plant Science 26(12): 1210-1212. DOI: 10.1016/j.tplants.2021.09.007.

http://www.aloki.hu ● ISSN 1589 1623 (Print) ● ISSN 1785 0037 (Online)
DOI: http://dx.doi.org/10.15666/aeer/2301_171188